Factors and Dynamics of Cu Nanocrystal Reconstruction under CO_2 Reduction

Wojciech T. Osowiecki[1,2], Jasper J. Nussbaum[1], Gaurav Kamat[1,3], Georgios Katsoukis[2], Marc Ledendecker[4], Heinz Frei[2], Alexis T. Bell[3], A. Paul Alivisatos[1,2,5,6]*

[1]Department of Chemistry, University of California, Berkeley, California 94720, USA.

[2]Molecular Biophysics and Integrated Bioimaging Division, Lawrence Berkeley National Laboratory, Berkeley, CA 94720, USA.

[3]Department of Chemical and Biomolecular Engineering, University of California, Berkeley, California 94720, USA.

[4]Department of Interface Chemistry and Surface Engineering, Max-Planck-Institut für Eisenforschung GmbH, Max-Planck-Straße 1, 40237 Düsseldorf, Germany

[5]Department of Materials Science and Engineering, University of California, Berkeley, California 94720, USA.

[6]Kavli Energy NanoScience Institute, Berkeley, California 94720, USA.

Abstract

The structure of Cu nanocrystals as catalysts for the electrochemical reduction of CO_2 is a subject of considerable contemporary interest. Recent efforts have focused mainly on the preparation of Cu nanocrystals, but the question of their stability is equally relevant and has not been considered as extensively. Herein, we report on the reconstruction of Cu nanocrystals during CO_2 reduction and discuss the factors influencing the observed changes with computer-based quantitative analysis and spectroscopic techniques. The timelines of opposing phenomena, sintering and declustering, previously reported separately, are detailed with a focus on two forces affecting the final morphology: applied potential and reaction intermediates. This intriguing system demonstrates the need for fundamental understanding of catalyst behavior preceding the ability to control its performance.

Main Body

For practical purposes, catalysts are judged not only by their initial selectivity and efficiency but also by their stability and performance over time. As catalysis is inherently a dynamic process, it is crucial to study catalyst degradation in order to improve process lifetime and uniformity of performance.[1,2] One of the most important reactions that call for the discovery of more robust and controllable materials is the electrochemical carbon dioxide reduction reaction (CO_2RR).[3] Over the last few years, significant effort has been devoted to the investigation of Cu-based catalysts that can convert carbon dioxide, a greenhouse gas, into useful fuels and chemicals, such as ethanol and ethylene, also known as C_{2+} products.[4] In the hope of achieving a near-unity conversion into specific CO_2RR targets, researchers often focus on nano-structured catalysts with high-energy facets and undercoordinated atoms,[5,6] but such morphologies come with inherent trade-offs. While under-coordinated atoms on the surface are desirable from the standpoint of activity and product selectivity, they are also most likely to be unstable with time and contribute to surface restructuring of the catalyst and a possible a loss of expected properties.[7] More recently, the restructuring and degradation during CO_2RR of Cu catalysts, both bulk[8,9] and nanoparticle systems,[10,11] have received greater attention. Nevertheless, the subject deserves additional study, as the researchers report significantly different behaviors. Starting with monodisperse Cu nanocrystals and very similar catalytic conditions, some groups observe sintering, i.e., cluster growth and surface area loss,[12,13] while other groups find evidence of declustering and surface area increase.[11,14]

In this work, we focus directly on the factors and the dynamics of Cu nanocrystal reconstruction as a result of CO_2RR, and we report evidence for both sintering and declustering

during the reaction. We study the morphological change of small (7 nm), relatively monodisperse (± 1.5 nm), Cu nanospheres bound with tetradecylphosphonate ligands on a glassy carbon electrode (Figures S1-2). This material was selected because its CO_2RR catalytic performance has been well-studied,[12,13] but the accompanying reconstructions, while observed, remain elusive and underexplored. By probing the surface of the electrode after various durations of catalysis, as well as methodically modifying the experimental parameters (nanoparticle loading, composition of the feed gas, pH), we have gained information about the evolution of particle sizes and shapes and some initial insights into possible mechanisms of these transformations. These studies show that particular attention must be given to the effects of carbon monoxide (CO), a primary intermediate formed during CO_2RR. As discussed previously, the applied potential alone can dramatically change the nanocrystal surface,[11] but the presence of CO_2RR intermediates, especially CO, results in vastly different particle size distributions (PSDs) and crystalline domains. Both sintering and declustering are observed. Crucially, these phenomena appear to occur at different timescales, and further work is needed to elucidate the complete reconstruction mechanisms and sequence.

CO_2RR was performed by applying a potential of -1.1V vs. reversible hydrogen electrode (RHE) in 0.1M $CsHCO_3$, common catalytic conditions optimized for C_{2+} products.[15,16] Cu nanocrystals (NCs) were spin-coated onto a glassy carbon substrate, and the loading was optimized between a sub-monolayer to a monolayer for the best imaging conditions (Figure 1). Each electrode was imaged using high-resolution scanning electron microscopy (SEM) before and after catalysis, which allowed for capturing the structural information on the original substrate, eliminating any risk of distortion associated with a transfer process. To ensure consistency in loading, identical-location imaging was performed (more details in SI) such that

the same spot on the electrode was imaged several times after various durations of CO_2RR.[17] Many previous reports on Cu NCs for CO_2RR include individual SEM images,[11–13] but one cannot infer precise size information or sample variability from one image. Therefore, we adapted a computer script to reproducibly identify material clusters, measure their size, and construct a PSD from thousands of individual data points (Figure 2).[18] As higher loadings were characterized by significant heterogeneity, we focused on the analysis of low loadings which displayed easier-to-fit spherical shapes and captured the overall reconstruction trends equally well. The quantitative approach is presented as a proof of concept, with the intention of demonstrating its promise in elucidating the reconstruction mechanism akin to earlier studies of thermal sintering.[19,20]

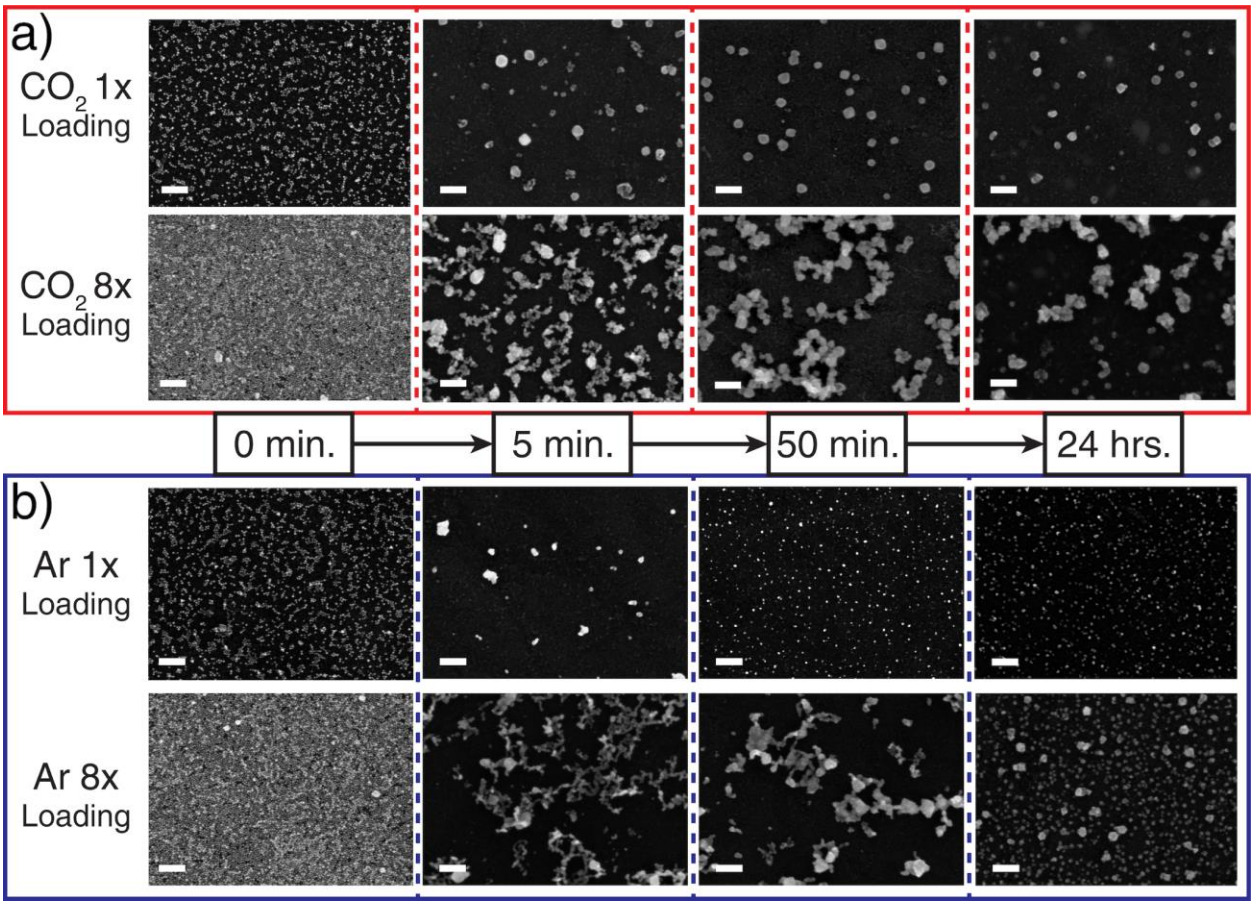

Figure 1. Identical-location SEM images of the Cu catalyst (1x and 8x loading) on the electrode before and after catalysis at -1.1 V vs. RHE in 0.1M $CsHCO_3$. *Electrocatalysis was performed in the presence of a) CO_2; b) argon. All scale bars correspond to 100nm. Magnified versions of the images located in the SI (Figures S3-10).*

The initial catalyst reconstruction occurs very quickly. After 5 min of CO_2RR, Cu NCs already change their size by sintering, i.e., loss of surface area (Figure 1a). While some particles assemble randomly, the other objects display much more uniform and spherical shape. After an additional 45 min, under reaction conditions, the morphology seems more defined, with the majority of the material having regular shapes that resemble cubes and spheres to different degrees. This distinction is perhaps most visible for the 8x loading (Figures 1a and S8-9) where

the finer particles and grains merge into larger structures with less contrast variation on the SEM. However, the growth *reverses* after the first hour of CO_2RR, and the resulting objects *decluster*. After 24 h, some clusters are even smaller than the original particle size (4-5 nm vs. 7 nm). Figure S11 captures the above-described behavior for three different loadings of Cu NCs (1x, 2x, 8x) and while there are sample-to-sample variations, the reconstruction trend always remains the same: nanoparticles join together to form larger, relatively uniform structures for the first hour of the reaction, but then, over time, shrink in size by declustering. When discussing the catalytic behavior of Cu NCs, previous reports either focus on sintering or declustering, but we have evidence to show that both phenomena occur, just on different timescales.

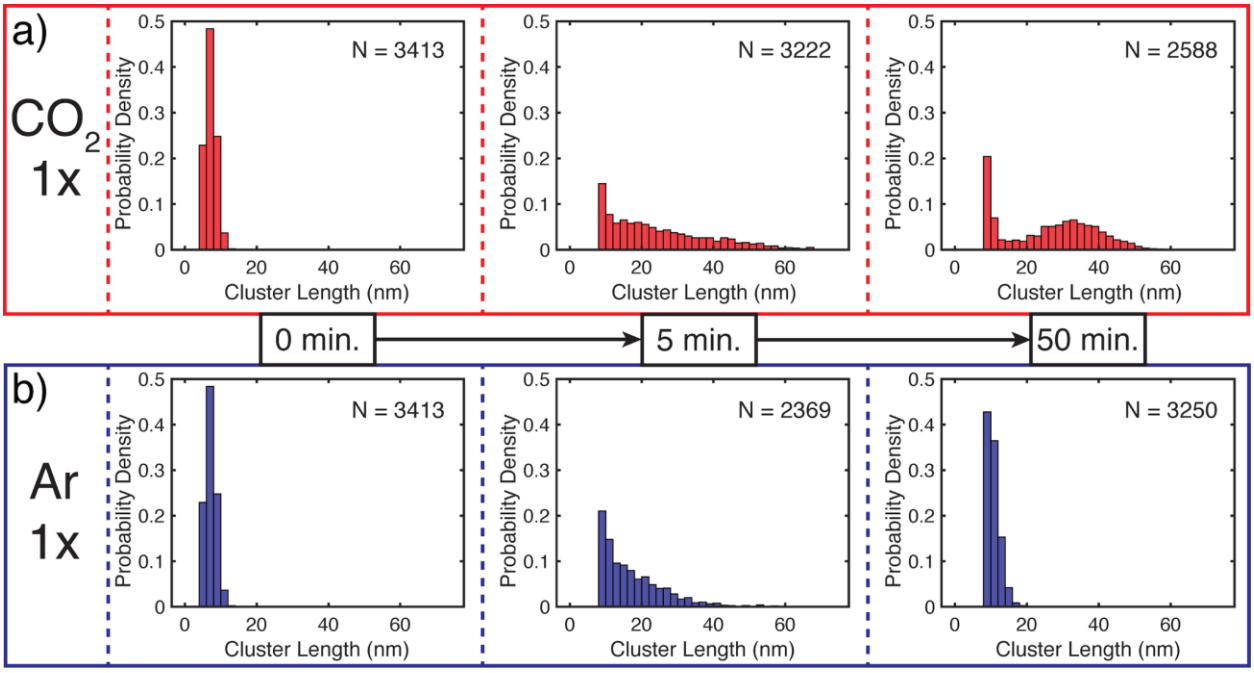

Figure 2. Particle size distribution of the Cu catalyst (1x loading) before and after catalysis at -1.1 V vs. RHE in a) CO_2 saturated and b) argon saturated 0.1M $CsHCO_3$. *The original size distribution for CO_2 and argon experiments is identical.*

To simplify the complex landscape of Cu NP reconstructions under CO_2RR, each factor of interest can be investigated separately with control experiments. Considering potential hypotheses for the causes of morphological change, three parameters were chosen: nanoparticle loading, pH, and the composition of the gas fed to the electrolyzer (CO_2 or Ar). Argon is a noble gas and should have no impact on the morphological change regardless of the applied potential, so it can serve as an appropriate control since the only reaction that will occur is the hydrogen evolution reaction (HER). As shown in Figures 1 and S11, nanoparticle loading does not appear to change the patterns of the reconstruction, only the timescales. Regarding pH during CO_2RR, it locally increases due to the production of OH^- ions and, in theory, Cu could transiently form copper hydroxide and then be redeposited as Cu.[21] This is unlikely at the applied potential but was considered as a hypothesis. Nevertheless, electrocatalysis in 0.1M KOH and argon demonstrates that even significantly higher pH alone does not reproduce the formation of such structures (Figure S12). Instead, particles form into thin irregular dendrites. The dendritic formations are characteristic of sintering through the process of particle migration and coalescence (PMC), commonly reported under reducing applied potential.[1,22]

Since electrolysis in high pH but without CO_2 does not result in the formation of any spherical clusters, this implies that CO_2 and its reaction intermediates play an essential role in Cu reconstruction. To verify this hypothesis, a series of experiments were conducted in the original $CsHCO_3$ buffer, sparged with argon before and during the catalysis. Indeed, without the presence of CO_2, NCs undergo a different morphological change (Figure 1b). Electrolysis in both CO_2 and argon bring the sintering into dendritic forms, likely a result of PMC, but the clusters from argon conditions never form individual crystalline grains larger than the starting material (Figure S9) or any spherical shapes, and they already begin to shrink within the first hour of electrocatalysis.

The differences between CO_2 and argon conditions are well captured by the PSDs (Figure 2). Importantly, the PSD after 5 min of electrolysis in argon displays a log-normal shape, which is characteristic of a PMC process.[19] The equivalent PSD for CO_2 electrolysis has an extended tail towards larger sizes, demonstrating that the CO_2RR reconstruction cannot be solely attributed to the applied potential and PMC.

To further investigate the morphological differences between clusters formed in the presence and the absence of CO_2RR intermediates, Cu structures were transferred for imaging with high-resolution transmission electron microscopy (HRTEM). This technique did not preserve the original arrangement of the material on the electrode but permitted a more precise analysis of individual clusters. As shown in Figures 1 and S3-10, CO_2RR reconstruction results in two types of structures: uneven patches of the original NCs and more spherical, larger shapes with little contrast variation in SEM. The former structures occur under argon electrolysis, but the latter do not. HRTEM confirms the relevance of these differences. While the individual crystalline domains after argon conditions are never larger than in the original 7 nm nanospheres, the presence of CO_2 during electrocatalysis leads to the formation of single grains extending for more than 30 nm (Figure 3). Notably, all of the observed material is Cu_2O, as the microscopy was performed *ex situ*, and Cu readily oxidizes in air.[23] This constitutes a limitation of the presented results, as it is not known exactly how the material looks *in operando*. Nevertheless, the reported changes in the morphology can be confidently ascribed to the presence of CO_2RR intermediates thanks to the control electrocatalysis performed under argon, when only adsorbed hydrogen is present on the surface during HER. Furthermore, the current measurements obtained *in situ* agree with the morphological changes observed by microscopy. As the observed current correlates with the surface area, we hypothesize that its initial decrease can be ascribed to

sintering and its subsequent increase to declustering (Figure S13). Cu material not exposed to CO_2RR undergoes faster and more extensive declustering (Figure 1), consistent with the trends in current seen for electrolysis conducted in CO_2 and argon.

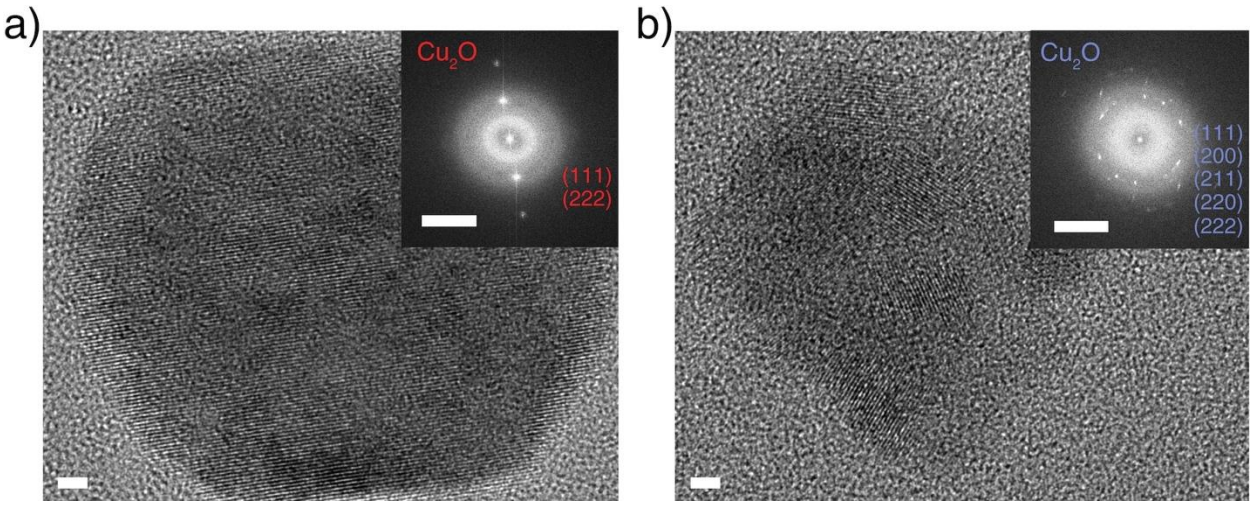

Figure 3. HRTEM images of individual Cu clusters after 50 min of catalysis in the presence of a) CO_2; b) argon. Scale bars correspond to 2 nm. Insets: FFT pattern identifying the material as Cu_2O (scale bar: 5 nm^{-1}).

Control experiments without either applied potential (Figure S14) or CO_2 (Figure 1b) confirm that both parameters are necessary for the production of spherical clusters with large single-crystal domains. Therefore, products of the electrochemical reduction of CO_2 play a crucial role in shaping the Cu NC reconstruction. It has been demonstrated that CO, the most abundant CO_2RR intermediate, can induce Cu reconstruction.[24,25] Indeed, electrocatalysis with CO instead of CO_2 yields similar spherical morphologies, corroborating the hypothesis of CO being the active species (Figure S15). Further insight comes from CO_2RR performed on Au NCs, which leads to dendritic growth, not unlike the morphology of Cu in argon conditions.[26] Since Au has much weaker binding affinity for CO than Cu does,[5] it implies that CO bonding is

responsible for the formation of clusters that cannot be solely attributed to the negatively polarized electrode. It remains less certain how the observed *ex situ* oxidized structures relate to the morphology under operating conditions. Thermodynamically, at -1.1V vs. RHE, Cu must be in the metallic state, and the oxidation to Cu_2O takes place at open circuit potential at the end of electrolysis and when in contact with the air.[27] Therefore, two hypotheses arise. Either CO increases the likelihood of large crystalline domain generation during catalysis, or it changes the way that the clusters oxidize at the end of the reaction and the larger grains form only after catalysis. Grain boundaries have been seen as crucial for the CO_2RR activity,[28] but the exact mechanism is still uncertain, and the dynamics of grain boundary formation have not been explored much.[29] Since CO demonstrates an intriguing propensity to modify crystalline domains either during the sintering process or during post-catalytic oxidation, this phenomenon should be probed further.

The loss of ligands stabilizing the original nanocrystals has also been proposed as a cause of the morphological change, especially sintering.[12] The reason might be the reductive desorption of the phosphonate ligands at negative potentials which has been reported before for long-chain alkanethiolates on gold substrates.[30] A bare metallic surface has higher surface energy than that covered by ligands, and therefore should be more mobile, driving towards particle growth. In this study, the presence of ligands before and after electrocatalysis is probed with two surface-sensitive techniques: infrared reflection-absorption spectroscopy (IRRAS) to detect C-H stretches from the alkyl chain with two main bands at 2915 cm^{-1} and 2846 cm^{-1}, and x-ray photoelectron spectroscopy (XPS) to detect the phosphorus atom in the binding group. The techniques combined demonstrate the loss of full ligand molecules, from the head to the tail, during CO_2RR (Figure 4). Such loss has been observed previously, but it was reported only in

absolute terms, not as concentration.[11,13,26] Fortunately, XPS offers more insight. Absolute Cu counts correlate well with the observed changes in the surface area during the first 60 min of catalysis, i.e., continuous sintering for CO_2 conditions vs. sintering and then declustering for argon conditions. Because of this, the increasing atomic ratio of P to Cu for the CO_2RR samples implies that the ligands may pack more densely during the sintering step, perhaps also influencing the morphology, along with CO. Finally, it is also worth noting that the Cu-O signal is stronger for CO_2 conditions, suggesting that CO exposure promotes Cu oxidation, presumably at open circuit potential after electrocatalysis.

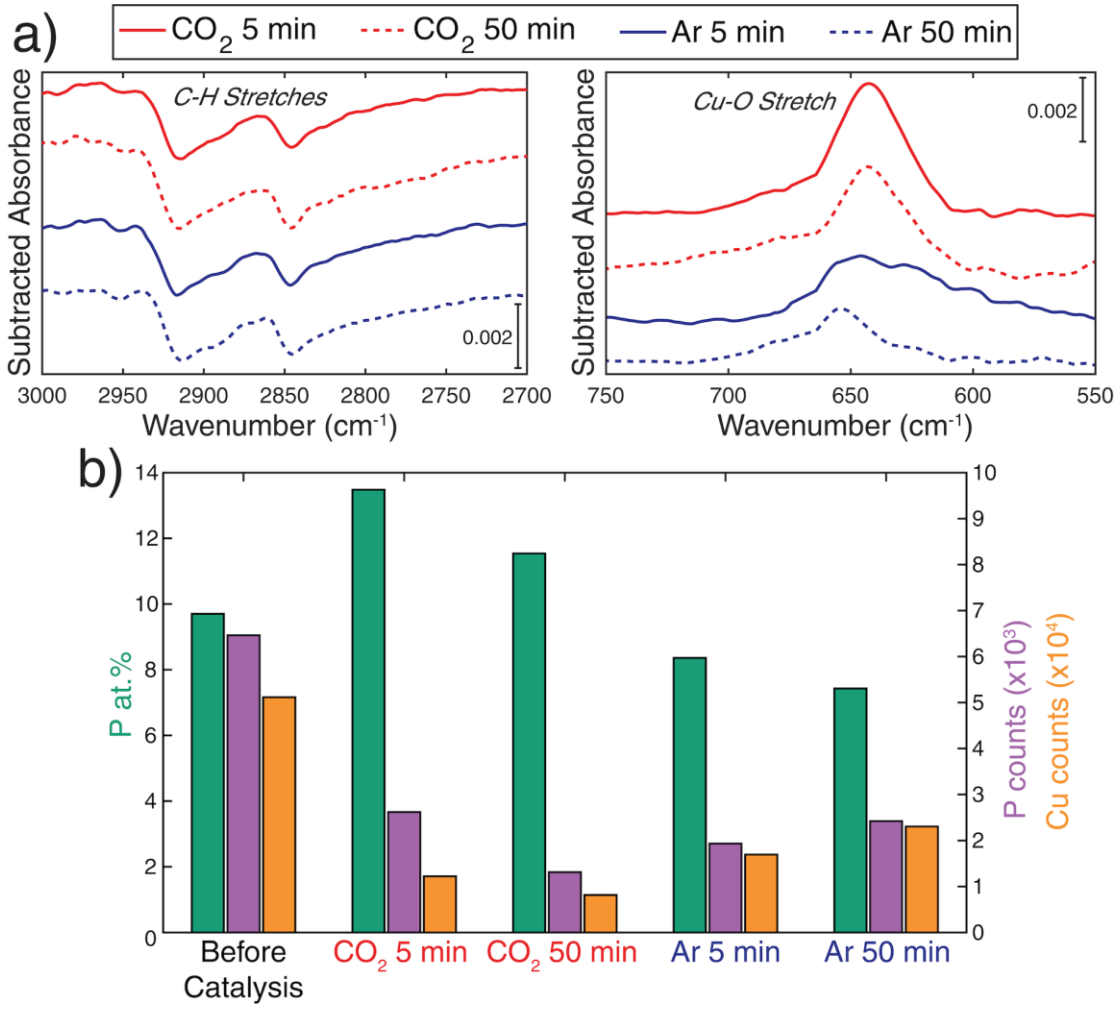

Figure 4. a) a) Subtracted IRRAS spectra showing the difference in absorption for samples after 5 min (continuous line) and after 50 min (dashed line) of chronoamperometric measurements at -1.1V vs. RHE in CO2 (red) and argon (blue) saturated 0.1M CsHCO3. The C-H region is displayed at the left while the Cu-O region at the right. Negative peaks indicate a loss of signal. b) Left axis: the elemental ratio of P to Cu reported in at.% and calculated from XPS data for the electrodes before and after catalysis. Right axis: absolute XPS counts for Cu and P used for the calculation of P at.%. The fitted spectra used for this calculation are shown in Figure S16. Cu counts correlate well with the observed surface area changes during the first 60 min of catalysis.

In summary, this work provides insights into the factors influencing the dynamics of Cu nanocrystal reconstruction under CO_2RR by investigating the effects of particle loading, the relevance of CO_2, and pH. Of these parameters, CO_2RR intermediates, most likely CO, demonstrate major relevance for the outcome of the morphological change. CO increases the propensity for the formation of larger, more spherical clusters with fewer crystalline domains as opposed to the finer, more dendritic structures caused solely by the negative polarization of the electrode, which induces PMC. The methodical *ex situ* identical-location SEM observations confirm the existence of both sintering and declustering, previously reported separately. These phenomena occur on different timescales, as particles first grow in size and later break apart, but declustering is slower under CO_2RR conditions, presumably due to some stabilizing role of CO. It is crucial to understand why the same catalytic conditions drive the PSDs into two opposite directions. The complex behavior calls for the existence of opposing forces, such as unfavorable surface energy of small Cu clusters versus favorable surface interactions with reaction intermediates, as recently discussed by Huang *et al*.[11] Clearly, more theoretical work, as well as

operando studies, need to be done. By describing this intriguing system, we hope to demonstrate the relevance of morphological studies that include quantitative computer-based approaches and spectroscopic information to the pursuit of improving the performance and stability of catalysts.

Associated content

Supporting information

Materials and synthesis; experimental and characterization procedures; magnified SEM images from Figure 1; miscellaneous supporting figures (further particle size distributions, SEM images of electrodes after various electrochemical conditions, chronoamperometry current measured during electrocatalysis, X-ray photoelectron spectroscopy spectra); discussion of the Matlab script used for the generation of particle size distribution (PDF)

Matlab code for particle size distribution generation and an example SEM image for analysis (ZIP)

Author Information

Corresponding Author

*paul.alivisatos@berkeley.edu

Acknowledgments

This work was supported by the U.S. Department of Energy, Office of Science, Office of Basic Energy Sciences, Materials Sciences and Engineering Division, under Contract No. DE-AC02-05-CH11231 within the Inorganic/Organic Nanocomposites Program (KC3104) and the Molecular Foundry. W.T.O was supported by the Siebel Scholarship from the Siebel Foundation.

The authors appreciate useful discussions with Ezra Clark, Colin Ophus, Chelsea Yang, Pratima Satish, Alex Powers, Colin Ophus, Adam Schwartzberg, Virginia Altoe, Miquel Salmeron, and Peter Lobaccaro.

References

(1) Goodman, E. D.; Schwalbe, J. A.; Cargnello, M. Mechanistic Understanding and the Rational Design of Sinter-Resistant Heterogeneous Catalysts. *ACS Catal.* **2017**, *7*, 7156–7173.

(2) Spöri, C.; Kwan, J. T. H.; Bonakdarpour, A.; Wilkinson, D. P.; Strasser, P. The Stability Challenges of Oxygen Evolving Catalysts: Towards a Common Fundamental Understanding and Mitigation of Catalyst Degradation. *Angew. Chemie - Int. Ed.* **2017**, *56*, 5994–6021.

(3) Montoya, J. H.; Seitz, L. C.; Chakthranont, P.; Vojvodic, A.; Jaramillo, T. F.; Nørskov, J. K. Materials for Solar Fuels and Chemicals. *Nat. Mater.* **2016**, *16*, 70–81.

(4) van de Lagemaat, J.; Sargent, E. H.; Kelley, S. O.; Tao, L.; Bushuyev, O. S.; Dinh, C. T.; De Luna, P.; Saur, G. What Should We Make with CO2 and How Can We Make It? *Joule* **2018**, *2*, 825–832.

(5) Li, Y.; Sun, Q. Recent Advances in Breaking Scaling Relations for Effective Electrochemical Conversion of CO2. *Adv. Energy Mater.* **2016**, *6*, 1600463.

(6) Chorkendorff, I.; Dickens, C. F.; Seh, Z. W.; Kibsgaard, J.; Jaramillo, T. F.; Nørskov, J. K. Combining Theory and Experiment in Electrocatalysis: Insights into Materials Design. *Science* **2017**, *355*, eaad4998.

(7) Moulijn, J. A.; Van Diepen, A. E.; Kapteijn, F. Catalyst Deactivation: Is It Predictable?

What to Do? *Appl. Catal. A Gen.* **2001**, *212*, 3–16.

(8) Kim, Y. G.; Baricuatro, J. H.; Javier, A.; Gregoire, J. M.; Soriaga, M. P. The Evolution of the Polycrystalline Copper Surface, First to Cu(111) and Then to Cu(100), at a Fixed CO2RR Potential: A Study by Operando EC-STM. *Langmuir* **2014**, *30*, 15053–15056.

(9) Gunathunge, C. M.; Li, X.; Li, J.; Hicks, R. P.; Ovalle, V. J.; Waegele, M. M. Spectroscopic Observation of Reversible Surface Reconstruction of Copper Electrodes under CO2 Reduction. *J. Phys. Chem. C* **2017**, *121*, 12337–12344.

(10) Grosse, P.; Gao, D.; Scholten, F.; Sinev, I.; Mistry, H.; Roldan Cuenya, B. Dynamic Changes in the Structure, Chemical State and Catalytic Selectivity of Cu Nanocubes during CO2 Electroreduction: Size and Support Effects. *Angew. Chemie - Int. Ed.* **2018**, *57*, 6192–6197.

(11) Huang, J.; Hörmann, N.; Oveisi, E.; Loiudice, A.; De Gregorio, G. L.; Andreussi, O.; Marzari, N.; Buonsanti, R. Potential-Induced Nanoclustering of Metallic Catalysts during Electrochemical CO2 Reduction. *Nat. Commun.* **2018**, *9*, 1–9.

(12) Manthiram, K.; Beberwyck, B. J.; Alivisatos, A. P. Enhanced Electrochemical Methanation of Carbon Dioxide with a Dispersible Nanoscale Copper Catalyst. *J. Am. Chem. Soc.* **2014**, *136*, 13319–13325.

(13) Kim, D.; Kley, C. S.; Li, Y.; Yang, P. Copper Nanoparticle Ensembles for Selective Electroreduction of CO2 to C2 – C3 Products. *Proc. Natl. Acad. Sci.* **2017**, *114*, 10560–10565.

(14) Hwang, Y. J.; Lee, S. Y.; Kim, C.; Won, D. H.; Lee, C. W.; Jung, H.; Oh, H.-S.; Cho, M. K.; Min, B. K. Electrochemical Fragmentation of Cu2O Nanoparticles Enhancing Selective C-C Coupling from CO2 Reduction Reaction. *J. Am. Chem. Soc.* **2019**, *141*,

4624–4633.

(15) Gao, D.; Arán-Ais, R. M.; Jeon, H. S.; Roldan Cuenya, B. Rational Catalyst and Electrolyte Design for CO2 Electroreduction towards Multicarbon Products. *Nat. Catal.* **2019**, *2*, 1–10.

(16) Resasco, J.; Chen, L. D.; Clark, E.; Tsai, C.; Hahn, C.; Jaramillo, T. F.; Chan, K.; Bell, A. T. Promoter Effects of Alkali Metal Cations on the Electrochemical Reduction of Carbon Dioxide. *J. Am. Chem. Soc.* **2017**, *139*, 11277–11287.

(17) Hodnik, N.; Zorko, M.; Bele, M.; Hočevar, S.; Gaberšček, M. Identical Location Scanning Electron Microscopy: A Case Study of Electrochemical Degradation of PtNi Nanoparticles Using a New Nondestructive Method. *J. Phys. Chem. C* **2012**, *116*, 21326–21333.

(18) Powers, A. S.; Liao, H. G.; Raja, S. N.; Bronstein, N. D.; Paul Alivisatos, A.; Zheng, H. Tracking Nanoparticle Diffusion and Interaction during Self-Assembly in a Liquid Cell. *Nano Lett.* **2017**, *17*, 15–20.

(19) Datye, A. K.; Xu, Q.; Kharas, K. C.; McCarty, J. M. Particle Size Distributions in Heterogeneous Catalysts: What Do They Tell Us about the Sintering Mechanism? *Catal. Today* **2006**, *111*, 59–67.

(20) Hansen, T. W.; Delariva, A. T.; Challa, S. R.; Datye, A. K. Sintering of Catalytic Nanoparticles: Particle Migration or Ostwald Ripening? *Acc. Chem. Res.* **2013**, *46*, 1720–1730.

(21) Kwon, Y.; Lum, Y.; Clark, E. L.; Ager, J. W.; Bell, A. T. CO2 Electroreduction with Enhanced Ethylene and Ethanol Selectivity by Nanostructuring Polycrystalline Copper. *ChemElectroChem* **2016**, *3*, 1012–1019.

(22) Behafarid, F.; Roldan Cuenya, B. Towards the Understanding of Sintering Phenomena at the Nanoscale: Geometric and Environmental Effects. *Top. Catal.* **2013**, *56*, 1542–1559.

(23) Lum, Y.; Ager, J. W. Stability of Residual Oxides in Oxide-Derived Copper Catalysts for Electrochemical CO 2 Reduction Investigated with 18 O Labeling. *Angew. Chemie - Int. Ed.* **2018**, *57*, 551–554.

(24) Eren, B.; Weatherup, R. S.; Liakakos, N.; Somorjai, G. A.; Salmeron, M. Dissociative Carbon Dioxide Adsorption and Morphological Changes on Cu(100) and Cu(111) at Ambient Pressures. *J. Am. Chem. Soc.* **2016**, *138*, 8207–8211.

(25) Eren, B.; Zherebetskyy, D.; Patera, L. L.; Wu, C. H.; Bluhm, H.; Africh, C.; Wang, L.-W.; Somorjai, G. A.; Salmeron, M. Activation of Cu(111) Surface by Decomposition into Nanoclusters Driven by CO Adsorption. *Science* **2016**, *351*, 475–478.

(26) Manthiram, K.; Surendranath, Y.; Alivisatos, A. P. Dendritic Assembly of Gold Nanoparticles during Fuel-Forming Electrocatalysis. *J. Am. Chem. Soc.* **2014**, *136*, 7237–7240.

(27) Garza, A. J.; Bell, A. T.; Head-Gordon, M. Is Subsurface Oxygen Necessary for the Electrochemical Reduction of CO2 on Copper? *J. Phys. Chem. Lett.* **2018**, *9*, 601–606.

(28) Feng, X.; Jiang, K.; Fan, S.; Kanan, M. W. A Direct Grain-Boundary-Activity Correlation for CO Electroreduction on Cu Nanoparticles. *ACS Cent. Sci.* **2016**, *2*, 169–174.

(29) Raciti, D.; Wang, C. Recent Advances in CO2 Reduction Electrocatalysis on Copper. *ACS Energy Lett.* **2018**, *3*, 1545–1556.

(30) Hobara, D.; Miyake, K.; Imabayashi, S.; Niki, K.; Kakiuchi, T. In-Situ Scanning Tunneling Microscopy Imaging of the Reductive Desorption Process of Alkanethiols on Au(111). *Langmuir* **1998**, *14*, 3590–3596.

For Table of Contents Only